We are IntechOpen, the world's leading publisher of Open Access books
Built by scientists, for scientists

6,900
Open access books available

186,000
International authors and editors

200M
Downloads

Our authors are among the

154
Countries delivered to

TOP 1%
most cited scientists

12.2%
Contributors from top 500 universities

CLARIVATE ANALYTICS
BOOK CITATION INDEX
INDEXED

WEB OF SCIENCE™

Selection of our books indexed in the Book Citation Index
in Web of Science™ Core Collection (BKCI)

Interested in publishing with us?
Contact book.department@intechopen.com

Numbers displayed above are based on latest data collected.
For more information visit www.intechopen.com

Physical Modeling of Gas Pollutant Motion in the Atmosphere

Ondrej Zavila

Additional information is available at the end of the chapter

1. Introduction

Air pollution is becoming an increasingly serious global issue. Factories produce large amounts of pollutants that damage the environment and harm human health. From this point of view, problems of motion and dispersion of pollutants in the atmosphere relate not only to environmental studies but also to other disciplines, such as safety engineering.

An understanding of the physical principles of pollutants' motion and dispersion is important in order to determine the impact of air pollution on the environment and humans. This study only deals with these physical principles of pollutants' motion and dispersion. Possible chemical reactions in the atmosphere are not covered.

For the purpose of the study, a simple model of a typical real situation was defined. Physical parameters of the model were gradually modified to achieve visible changes in results so that general principles could be defined. The above-mentioned demonstration model represents a chimney situated in a simple flat terrain. Gas pollutant is discharged from the chimney and carried by flowing air. Gas pollutant plume is detected and visualized with a numerical model as iso-surfaces or contours of pollutant concentrations in two-dimensional cut planes of three-dimensional geometry.

The dependence of the pollutant plume shape, size and inclination on modification of three physical parameters was investigated. The selected parameters included pollutant density, air flow velocity and model scale.

The results are presented in the form of text, commented figures and tables. ANSYS Fluent 13.0 CFD (Computational Fluid Dynamics) code was used to demonstrate and visualize all problem variants (see [1],[2]). The numerical model of the pollutant plume motion created in this software had been verified by an experiment conducted in the low-speed wind tunnel in the Aerodynamic Laboratory of the Academy of Sciences of the Czech Republic in Novy

Knin (see [3],[4],[5]). One of the aims of the study is also to demonstrate that physical modeling of pollutant plume motion and dispersion with severely downscaled models has its limitations that should be known and considered to avoid obtaining false results.

2. Physical modeling in wind tunnels

Wind tunnels are facilities where specific air flow regime can be set up with a certain level of precision as required by investigators. They are primarily used to study aerodynamic characteristics of bodies. The history of wind tunnels dates back to 1751 and is connected with the name of Francis H. Wenham, a Council Member of the Aeronautical Society of Great Britain. In the beginning, wind tunnels were used mainly in aviation development. Nowadays, they are used for many applications in, for instance, automotive industry, building industry, environmental and safety engineering.

Wind tunnels can be classified, for example, by the velocity of air flow (see [6]) as:

a. *Low-speed wind tunnels* – air flow velocity in the measuring section of the tunnel is low enough to consider the air as an incompressible medium;
b. *High-speed wind tunnels* – air flow velocity in the measuring section of the tunnel is high enough to consider the air as a compressible medium;
c. *Subsonic wind tunnels* - air flow velocity in the measuring section of the tunnel is high enough (subsonic) to consider the air as a compressible medium;
d. *Supersonic wind tunnels* - air flow velocity in the measuring section of the tunnel is high enough (supersonic) to consider the air as a compressible medium.

Except for applications using only clean air, there are many applications in which various pollutants are applied. Pollutants are introduced to visualize the air flow field or to simulate the motion and dispersion of pollution in the real atmosphere. These applications can be found, for example, in environmental and safety engineering. Results of measurements using downscaled models in wind tunnels can be used as base data for local emergency planning studies.

2.1. Criteria of physical similarity

Two phenomena can be considered to be similar (despite different geometrical scales) if three types of similarity match: geometric, kinematic and dynamic. Criteria of geometric similarity require that the ratios of main corresponding dimensions on the model and the original pattern be constant. Also, main corresponding angles on the original pattern and the model must be of the same value. Criteria of kinematic similarity require that the ratios of velocities at corresponding points be the same for both the original pattern and the model. Criteria of dynamic similarity require that the ratios of the main forces at corresponding points be the same for both the original pattern and the model.

Forces can be divided into two groups: areal forces and volume (weight) forces. Areal forces include friction forces, compression forces, and capillary (surface) forces. Volume (weight)

forces include inertial forces, gravity forces and impulse forces (resulting from the change in momentum). According to the type of phenomena, these forces can be put into mathematical relation and criteria (numbers) of similarity can be established. In fluid mechanics, the Reynolds number, Euler number, Newton number, Froude number, Weber number, and Mach number are the most widely known criteria. Each of them expresses ratio between two different forces. In practice, it is not possible to achieve correspondence between the original pattern and the model in all criteria. Therefore, it is always up to the investigators who must use their knowledge and experience to choose the right and most important criterion (or criteria) for the investigated phenomenon. As a result, investigators usually work with one or two dominant criteria of similarity [7],[8],[9].

2.2. Applying froude number

The Froude number expresses the ratio between gravity forces and inertial forces. Gravity forces cause vertical movements of the plume (climbing or descending) and inertial forces cause horizontal movements of the plume. The Froude number can be therefore considered as a criterion of dynamic similarity, which should be of the same value for both the scaled model and the real pattern (see [7],[8],[9]).

The Froude number can be defined as

$$Fr \approx \frac{F_{I-air}}{F_{G-pollutant}} = \frac{\rho_{air} \cdot S \cdot v_{air}^2}{\rho_{pollutant} \cdot g \cdot V} = \frac{\rho_{air} \cdot l_2 \cdot l_3 \cdot v_{air}^2}{\rho_{pollutant} \cdot g \cdot l_1 \cdot l_2 \cdot l_3} = \frac{\rho_{air} \cdot v_{air}^2}{\rho_{pollutant} \cdot g \cdot l_1} \qquad (1)$$

where F_{I-air} is the inertial force due to the air acting on pollutant element [N], $F_{G-pollutant}$ is the gravity force acting on pollutant element [N], ρ_{air} is the air density [kg/m³], $\rho_{pollutant}$ is the pollutant density [kg/m³], S is the surface of pollutant element acted on by the flowing air [m²], v_{air} is the air flow velocity [m/s], g is the gravity acceleration constant [m/s²], V is the volume of pollutant element released from the pollutant source per 1 second [m³], l_1 is the 1st characteristic dimension of the pollutant source (length of pollutant cubic element) [m], l_2 is the 2nd characteristic dimension of the pollutant source (width of pollutant cubic element) [m] and l_3 is the 3rd characteristic dimension of the pollutant source (height of pollutant cubic element) [m]. l_3 can be replaced by $v_{pollutant}$ that represents the velocity of the pollutant released from the source in vertical direction [m/s]. Fr is a dimensionless constant [-] whose value determines whether the inertial force or the gravity force will dominate in the specific pollutant plume motion scenario.

All important characteristics are illustrated in Figure 1. Pollutant element was simplified into a rectangular cuboid with dimensions of l_1, l_2 and l_3 to make practical calculations easier. Of course, the spout of a real chimney can be of a different shape, most commonly circular or elliptical. In this case it is advisable to calculate the surface of the spout and transform the shape into a square or a rectangle with dimensions of l_1 and l_2. The value of l_3 remains the same (despite the shape of the spout) and is replaced by the velocity with which the pollutant leaves the source in vertical direction $v_{pollutant}$.
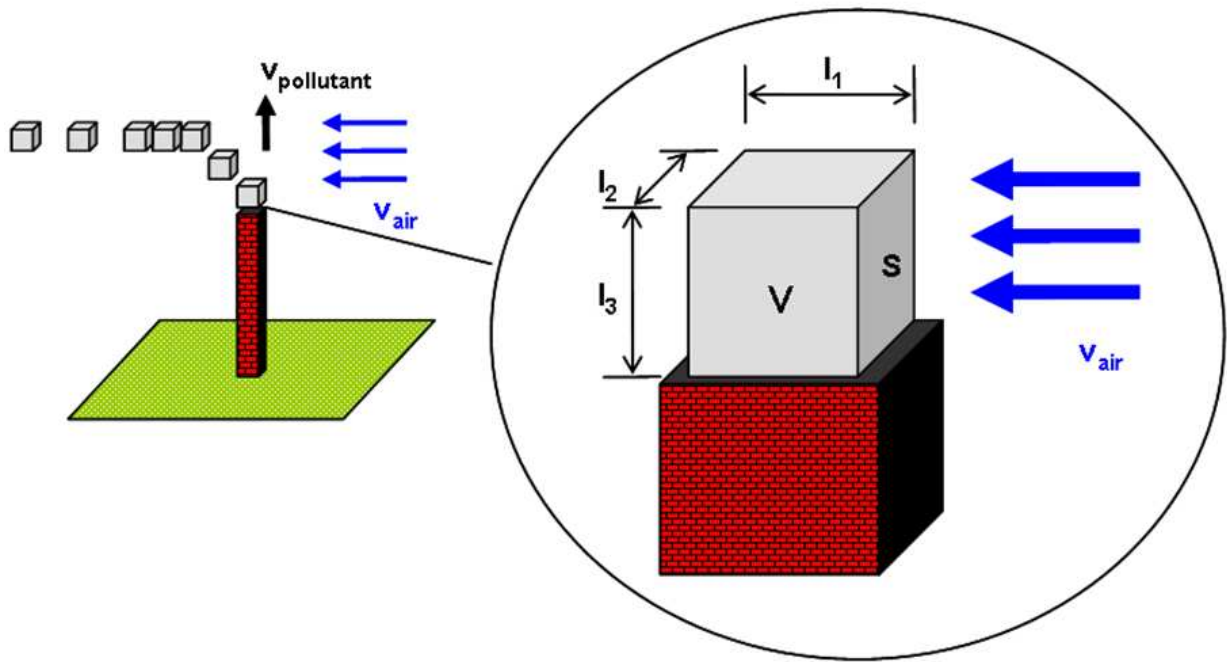
Figure 1. Air flow action on gas pollutant element leaking from the nozzle (chimney)

If $Fr < 1$, gravity forces are assumed greater than inertial forces. Hence, vertical motions (climbing or descending) of the gas pollutant plume can be expected due to different densities of the pollutant and the air. Plumes of light gas pollutants will tend to climb, whereas plumes of heavy gas pollutants will tend to descend.

If $Fr = 1$, gravity forces are assumed equal to inertial forces. Hence, gas pollutant plumes are carried by flowing air along with manifesting partial vertical motions.

If $Fr > 1$, inertial forces are assumed greater than gravity forces. Hence, vertical motions of the gas pollutant plume are limited or nonexistent. The gas pollutant plume is carried by strong flowing air, regardless of the pollutant—air density difference or weight of the pollutant.

This third scenario causes common difficulties when planning gas pollutant plume motion and dispersion experiments with downscaled models in low-speed wind tunnels. At small dimensions of measuring sections of common wind tunnels and, thus, low scales of models, the air flow may be too great to allow vertical motions of gas pollutant plumes. Proper conditions often cannot be assured in such cases.

2.3. Influence of air velocity

According to Equation (1) in Section 1.2, the air flow velocity v_{air} influences the inertial force F_{I-air} that causes gas pollutant horizontal motion. If all the other physical characteristics are constant, the following principles can be formulated: The greater the air flow velocity v_{air} is, the greater the inertial force F_{I-air} is. The greater the inertial force is, the more limited the pollutant plume vertical motions (climbing or descending) are.

The air flow velocity $v_{air, Fr=1}$ for $Fr = 1$ (i.e., inertial and gravity forces are equal) can be deduced from Equation (1) mentioned in Section 1.2:

$$1 = \frac{F_{I-air}}{F_{G-pollutant}} = \frac{\rho_{air} \cdot S \cdot v_{air, Fr=1}^2}{\rho_{pollutant} \cdot g \cdot V} = \frac{\rho_{air} \cdot l_2 \cdot l_3 \cdot v_{air, Fr=1}^2}{\rho_{pollutant} \cdot g \cdot l_1 \cdot l_2 \cdot l_3} = \frac{\rho_{air} \cdot v_{air, Fr=1}^2}{\rho_{pollutant} \cdot g \cdot l_1} \tag{2}$$

Thus, the air flow velocity $v_{air, Fr=1}$ is

$$v_{air, Fr=1} = \sqrt{\frac{\rho_{pollutant} \cdot g \cdot l_1}{\rho_{air}}} = \sqrt{\frac{\rho_{pollutant} \cdot g \cdot l_1 \cdot l_2 \cdot l_3}{\rho_{air} \cdot l_2 \cdot l_3}} = \sqrt{\frac{\rho_{pollutant} \cdot g \cdot V}{\rho_{air} \cdot S}} \tag{3}$$

However, one must realize that the change in air flow velocity influences also air flow field turbulent characteristics. For example, turbulent intensity is influenced when the air flows around solid objects or in a complex terrain. Investigators must consider whether these changes have a serious impact on accuracy of the experiment or mathematical model. This is very important for modeling gas pollutant motion and dispersion in a complex geometry (complex terrain) where the real model of turbulent flow field is the key element of the simulation. If the air turbulent flow field is seriously influenced by the change in the air flow velocity, the results of the analysis can be misleading. This approach is therefore not suitable for such cases and a different parameter of the model must be changed (see Sections 1.4 and 1.5).

2.4. Influence of pollutant density

According to Equation (1) in Section 1.2, the pollutant density $\rho_{pollutant}$ influences the gravity force $F_{G-pollutant}$ that causes gas pollutant vertical motions (climbing or descending). If all the other physical characteristics are constant, the following principles can be formulated: If the pollutant density $\rho_{pollutant}$ is greater than the air density ρ_{air}, the pollutant tends to descend (i.e., the gas pollutant plume descends). If the pollutant density $\rho_{pollutant}$ is lower than the air density ρ_{air}, the pollutant tends to climb (i.e., the gas pollutant plume climbs). The greater the gravity forces $F_{G-pollutant}$ are, the more significant the gas pollutant plume vertical movements (climbing or descending) are.

The pollutant density $\rho_{pollutant, Fr=1}$ for $Fr = 1$ (i.e., inertial and gravity forces are equal) can be deduced from Equation (1) in Section 1.2:

$$1 = \frac{F_{I-air}}{F_{G-pollutant}} = \frac{\rho_{air} \cdot S \cdot v_{air}^2}{\rho_{pollutant, Fr=1} \cdot g \cdot V} = \frac{\rho_{air} \cdot l_2 \cdot l_3 \cdot v_{air}^2}{\rho_{pollutant, Fr=1} \cdot g \cdot l_1 \cdot l_2 \cdot l_3} = \frac{\rho_{air} \cdot v_{air}^2}{\rho_{pollutant, Fr=1} \cdot g \cdot l_1} \tag{4}$$

Thus, the pollutant density $\rho_{pollutant, Fr=1}$ is

$$\rho_{pollutant, Fr=1} = \frac{\rho_{air} \cdot v_{air}^2}{g \cdot l_1} = \frac{\rho_{air} \cdot v_{air}^2 \cdot l_2 \cdot l_3}{g \cdot l_1 \cdot l_2 \cdot l_3} = \frac{\rho_{air} \cdot v_{air}^2 \cdot S}{g \cdot V} \tag{5}$$

A change in pollutant density in order to achieve the optimum ratio between inertial and gravity forces would be often the ideal solution. However, there is a problem. The densities of pollutants range within a narrow interval—approximately of one of order of magnitude—which is usually is not enough to compensate the Froude number differences resulting from, e.g., a substantial change of the model scale.

A typical example can be the physical modeling of gas pollutant plumes in low-speed wind tunnels where the scale of the model is around 1:1000. In such a case, there is a need to change the pollutant density 100, or even 1000 times, which is impossible. This is why change in pollutant density can be used to achieve only a small change in the Froude number. These small changes, however, may not be sufficient for a successful execution of the experiment or numerical modeling.

The change of the flowing gas density could be an alternative solution. For example, air could be replaced by a different gas with a different value of density. However, this change influences turbulent flow field characteristics, which may be undesirable (see Section 1.3).

2.5. Influence of model scale

According to Equation (1) in Section 1.2, the model scale can be expressed by using the value l_1 that represents the 1st characteristic dimension of the pollutant source (i.e., length of pollutant cubic element) (see Figure 1). The model scale influences both inertial and gravity forces and changes their ratio. If all the other physical characteristics are constant, the following principles can be formulated: The greater the model scale is, the greater the influence of gravity forces is. The smaller the model scale is, the greater the influence of inertial forces is. Gravity forces are, e.g. , greater in a model scaled at 1:4 than in that scaled at 1:1000 (see Section 2.6).

The value of the 1st characteristic dimension of the pollutant source (length of pollutant cubic element) $l_{1, Fr=1}$ for $Fr = 1$ (inertial and gravity forces are equal) can be deduced from Equation (1) in Section 1.2:

$$1 = \frac{F_{I-air}}{F_{G-pollutant}} = \frac{\rho_{air} \cdot S_{Fr=1} \cdot v_{air}^2}{\rho_{pollutant} \cdot g \cdot V_{Fr=1}} = \frac{\rho_{air} \cdot l_{2, Fr=1} \cdot l_{3, Fr=1} \cdot v_{air}^2}{\rho_{pollutant} \cdot g \cdot l_{1, Fr=1} \cdot l_{2, Fr=1} \cdot l_{3, Fr=1}} \quad (6)$$

or

$$1 = \frac{F_{I-air}}{F_{G-pollutant}} = \frac{\rho_{air} \cdot v_{air}^2}{\rho_{pollutant, Fr=1} \cdot g \cdot l_{1, Fr=1}} \quad (7)$$

Thus, $l_{1, Fr=1}$ is

$$l_{1, Fr=1} = \frac{\rho_{air} \cdot v_{air}^2}{\rho_{pollutant} \cdot g} = \frac{\rho_{air} \cdot v_{air}^2 \cdot l_{2, Fr=1} \cdot l_{3, Fr=1}}{\rho_{pollutant} \cdot g \cdot l_{2, Fr=1} \cdot l_{3, Fr=1}} = \frac{\rho_{air} \cdot v_{air}^2 \cdot S_{Fr=1}}{\rho_{pollutant} \cdot g \cdot S_{Fr=1}} \quad (8)$$

T model scale $M_{Fr=1}$ [-] for $Fr = 1$ (inertial and gravity forces are equal) is given by

$$M_{Fr=1} = \frac{1}{X} \tag{9}$$

where

$$X = \frac{l_1}{l_{1,\,Fr=1}} \tag{10}$$

The value l_1 represents the 1st characteristic dimension of the pollutant source (length of pollutant cubic element) in the original model. The value $l_{1,\,Fr=1}$ is the 1st characteristic dimension of the pollutant source in the model where $Fr = 1$ (i.e., inertial and gravity forces are equal).

If the model scale is changed, the change of the inertial force is given by

$$F_{I1} = X^2 \cdot F_{I2} \tag{11}$$

and the change of the gravity force is given by

$$F_{G1} = X^3 \cdot F_{G2} \tag{12}$$

The value X is a model scale factor [-]. If $X > 1$, the model is smaller than its original pattern (i.e., the model is downscaled). If $X < 1$, the model is larger than its original pattern (i.e., the model is enlarged). Equations (11) and (12) are deduced from Equation (1) for the Froude number. The situation is illustrated in Figure 2.
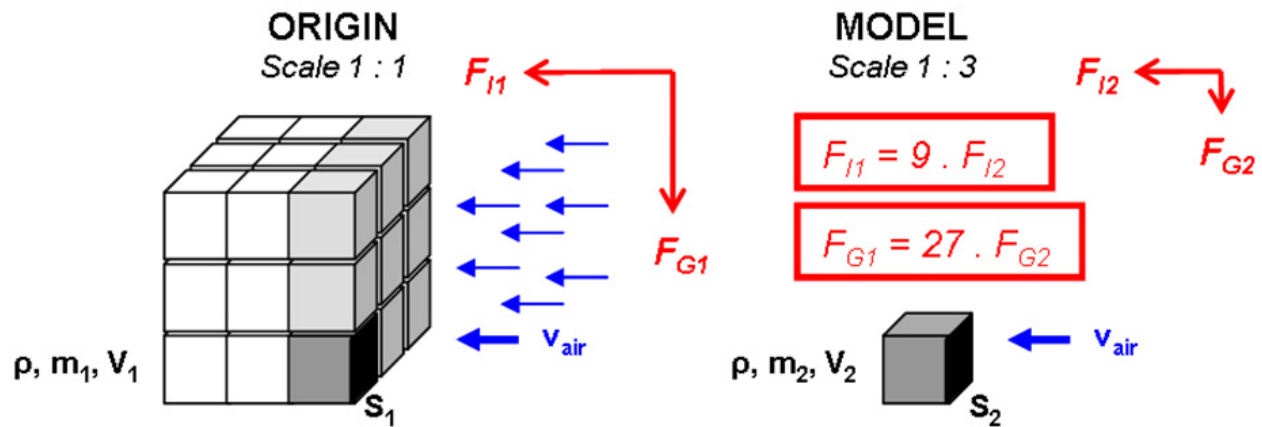

Figure 2. Inertial and gravity forces acting on gas pollutant element in two different model scales

A change in model scale always causes a change in the ratio of inertial and gravity forces. Therefore, some problems cannot be reliably modeled at other than approximately original scales. The range of deviation from the original depends on the discretion of investigators. Investigators must decide whether the tolerance of the results is acceptable.

Modeling of gas pollutant plume motions with severely downscaled models is a typical example of this problem. Downscaled pollutant plume models will not correspond to the originally scaled patterns without modifying some key physical characteristics (air flow velocity, turbulent characteristics, etc.).

The problem can be solved by using a numerical mathematical model verified by a clearly defined experiment of the same type of physical phenomenon. Once the numerical model is verified, it can be used for numerical simulation of any problem of the same physical principles, whatever the model scale is. Sometimes it is impossible to do the same with a physical experiment.

It can be concluded that severely downscaled experiments are not suitable for modeling gas pollutant plume motions because of possible absence of vertical movements. It is more advisable to use physical experiment data only for verification of the numerical mathematical model (code, software).

3. CFD numerical modeling of gas pollutant motion

CFD (Computational Fluid Dynamics) is an abbreviation for a category of sophisticated mathematical codes for fluid mechanics computations. These codes offer a wide range of applications including modeling of turbulent fluid flows, heat transfers, and species motions with or without chemical reactions. It is an effective tool for prediction and reconstruction of many physical phenomena, especially in mechanical engineering, civil engineering, safety engineering, power engineering, environmental engineering, and in many other disciplines.

3.1. CFD numerical modeling basics

CFD (Computational Fluid Dynamic) codes are based on the numerical solution of systems of partial differential equations that express the law of conservation of mass (continuity equation), the law of conservation of momentum (Navier-Stokes equations) and the law of conservation of energy (energy equation). This basic set of equations can be supplemented by additional equations that express heat transfer (heat transfer equations – convection, conduction or radiation), or species transport (species transport equations – gas, liquid or solid). The system of equations is then solved with an appropriate numerical method.

At the start of the modeling process, the geometrical shape of a two- or three-dimensional geometry is created that represents the object of modeling and its close surroundings. The size and shape of the geometry must enable the investigated phenomena to be captured.

In the second step, the geometry is covered with a grid. The grid divides the geometry into a finite number of two- or three-dimensional elements (cells) of a certain shape in which relevant physical quantities will be calculated. The quantities are calculated at the middle of the cells. Values in intermediate spaces are interpolated or extrapolated. The type and quality of grid influence the calculation time and the quality of results. A quality grid is smooth enough to capture the modeled phenomenon and its cells have as little shape deformation as possible compared to the ideal original shape.

In the third step, investigators choose the most suitable mathematical model and sub-models for the calculation of the problem. For gas pollutant plume motion and dispersion, the model of turbulence for the air flow field calculation is chosen first, than the species transport model is chosen for species transport modeling.

In the fourth step, boundary and initial conditions are defined. Boundary conditions are physical constants or variables that characterize the physical conditions at the boundaries of the geometry, i.e., at its inlet, outlet or walls. Boundary conditions do not change during the course of the calculation. They can be defined as a constant, a spatial-dependent function or a time-dependent function (polynomial, linear or periodic). Initial conditions are physical constants or variables that characterize the initial state of the system. Unlike boundary conditions, the initial conditions change in the course of the calculation after each iteration. If data for setting initial conditions are missing, at least approximate values should be entered. Initial conditions influence the calculation run-time, i.e., the time required to reach convergence.

In the fifth step, investigators set mathematical parameters of the calculation, e.g., solution schemes, under-relaxation parameters, and criteria of convergence. If required, as in case of calculations of time-dependent problems, special post-processing functions are set in this step, too.

Afterwards, the calculation is started and its progress monitored. Lastly, results are evaluated with available standard software tools or with preset post-processing functions (animations, time-dependent progress of physical variables, etc.) (see [1],[2]).

3.2. Basic equations

The following equations are used for basic air flow field calculations:

Continuity equation for compressible fluid flow

The continuity equation expresses the law of conservation of mass. For unsteady (time-dependent) compressible fluid flows, it can be written as a differential equation in form of

$$\frac{\partial \rho}{\partial t} + \frac{\partial \left(\rho \cdot \overline{u}_j \right)}{\partial x_j} = 0 \tag{13}$$

where ρ is the fluid density [kg/m³], t is time [s], $\overline{u}_j$ is the time-averaged j-coordinate of the fluid flow velocity [m/s], and x_j is a coordinate of the Cartesian coordinate system [-].

Equations for compressible fluid flow

These equations—known as Navier-Stokes equations—express the law of conservation of momentum. For calculating turbulent flows, time-averaged values must be applied. The substitution of the time-averaged values into the Navier-Stokes equations gives the Reynolds equations. The equation of conservation of momentum for compressible fluids can be written in the form corresponding to that in differential form as

$$\frac{\partial\left(\rho\cdot\overline{u}_i\right)}{\partial t}+\frac{\partial\left(\rho\overline{u}_i\cdot\overline{u}_j\right)}{\partial x_j}=-\frac{\partial\overline{p}}{\partial x_i}+\frac{\partial}{\partial x_j}\cdot\tau_{ji}+\rho\cdot\delta_{i3}\cdot g+\rho\cdot f_c\cdot\varepsilon_{ij3}\cdot\overline{u}_j+\rho\cdot f_j \qquad (14)$$

where ρ is the fluid density [kg/m³], t is time [s], $\overline{u}_j$ is the time-averaged j-coordinate of the fluid flow velocity [m/s], x_j is a coordinate of the Cartesian coordinates system [-], $\overline{p}$ is the time-averaged value of pressure [Pa], τ_{ji} is the tensor of viscous stress [Pa], δ_{i3} is the Kronecker delta [-], ε_{ij3} is the unit tensor for centrifugal forces [-], f_j is the j-coordinate of force [N], and g is the gravity acceleration [m/s²] (if gravity forces are included).

The meaning of terms in Equation (14):

1ˢᵗ term on the left	…………………	Unsteady term (acceleration)
2ⁿᵈ term on the left	…………………	Convective term
1ˢᵗ term on the right	…………………	Influence of pressure forces
2ⁿᵈ term on the right	…………………	Influence of viscous stress
3ʳᵈ term on the right	…………………	Influence of gravity forces (buoyancy)
4ᵗʰ term on the right	…………………	Influence of Earth rotation (Coriolis force)
5ᵗʰ term on the right	…………………	Influence of volumetric forces

The equation of turbulent kinetic energy k and the equation of turbulent dissipation rate ε are used to express the turbulent flow field variables. The exact equation for k can be deduced from the Navier-Stokes equations and written as

$$\frac{\partial k}{\partial t}+\frac{\partial\overline{u}_j\cdot k}{\partial x_j}=-\frac{\partial}{\partial x_j}\cdot\left[\overline{u'_j\cdot\left(\frac{u'_l\cdot u'_l}{2}+\delta_{jl}\cdot\frac{p'}{\rho}\right)}\right]+v_t\cdot\frac{\partial^2 k}{\partial x_j^2}-\overline{u'_l\cdot u'_j}\cdot\frac{\partial\overline{u}_l}{\partial x_j}-v\cdot\overline{\frac{\partial u'_l}{\partial x_j}\cdot\frac{\partial u'_l}{\partial x_j}} \qquad (15)$$

where k is the turbulent kinetic energy [m²/s²], t is time [s], $\overline{u}_j$ is the time-averaged j-coordinate of the fluid flow velocity [m/s], x_j is a coordinate of the Cartesian coordinate system [-], ρ is the fluid density [kg/m³], p' is a component of the pressure fluctuation [Pa], and v_t is the turbulent kinematic viscosity [Pa.s].

The meaning of terms in Equation (15):

1ˢᵗ term on the left	…………………	Turbulent energy rate
2ⁿᵈ term on the left	…………………	Convective transport of turbulent energy
1ˢᵗ term on the right	…………………	Turbulent diffusion due to pressure and velocity fluctuation
2ⁿᵈ term on the right	…………………	Molecular diffusion
3ʳᵈ term on the right	…………………	Production of turbulent kinetic energy due to sliding friction
4ᵗʰ term on the right	…………………	Viscous dissipation

The turbulent kinetic energy k from Equation (15) is

$$k = \frac{1}{2} \cdot \left(\overline{u_1'^2} + \overline{u_2'^2} + \overline{u_3'^2} \right) = \frac{1}{2} \cdot \overline{u_j'^2} \qquad (16)$$

where $\bar{u}_j$ represents time-averaged flow velocity components [m/s].

The exact equation for ε can be deduced from the Navier-Stokes equations and written as

$$\frac{\partial \varepsilon}{\partial t} + \frac{\partial \bar{u}_j \cdot \varepsilon}{\partial x_j} = \frac{\partial}{\partial x_j} \cdot \left(\frac{\nu_t}{\sigma_\varepsilon} \cdot \frac{\partial \varepsilon}{\partial x_j} \right) + C_{1\varepsilon} \cdot \nu_t \cdot \left(\frac{\partial \bar{u}_j}{\partial x_l} + \frac{\partial \bar{u}_l}{\partial x_j} \right) \cdot \frac{\partial \bar{u}_l}{\partial x_j} - C_{2\varepsilon} \cdot \frac{\varepsilon^2}{k} \qquad (17)$$

where ε is the turbulent dissipation rate [m²/s³], t is time [s], $\bar{u}_j$ is the time-averaged j-coordinate of the fluid flow velocity [m/s], x_j is a coordinate of the Cartesian coordinate system [-], ν_t is the turbulent kinematic viscosity [m²/s], σ_ε, $C_{1\varepsilon}$ and $C_{2\varepsilon}$ are empirical constants [-], and k is the turbulent kinetic energy [m²/s²].

The turbulent kinetic viscosity ν_t is

$$\nu_t = C_\nu \cdot \frac{k^2}{\varepsilon} \qquad (18)$$

where C_ν is an empirical constant [-].

Energy equation

The energy equation expresses the law of conservation of energy. According to this law, change in the total fluid energy $\bar{E}$ in the volume V is determined by the change of the inner energy and kinetic energy, and by the flux of both energies through surface S [m²] that surrounds volume V [m³]. The final equation can be written as

$$\frac{\partial}{\partial t} \cdot \left[\rho \cdot \bar{E} \right] + \frac{\partial}{\partial x_j} \cdot \left[\rho \cdot \bar{u}_j \cdot \bar{E} \right] = \rho \cdot \bar{u}_j \cdot f_j - \frac{\partial \left(p \cdot \bar{u}_j \right)}{\partial x_j} + \frac{\partial \left(\tau_{ji} \cdot \bar{u}_j \right)}{\partial x_l} - \frac{\partial \bar{q}_j}{\partial x_j} \qquad (19)$$

where t is time [s], ρ is the fluid density [kg/m³], $\bar{E}$ is the time-averaged value of energy [J/kg], $\bar{u}_j$ is the time-averaged j-coordinate of the flow field velocity [m/s], x_j is a coordinate of the Cartesian coordinate system [-], p is the pressure [Pa], τ_{ji} is the tensor of viscous stress [Pa], and $\bar{q}_j$ is the time-averaged j-coordinate of heat flux [J/(m².s)].

The meaning of terms in Equation (19):

1st term on the left	…………………	Energy rate
2nd term on the left	…………………	Convective transport of energy
1st term on the right	…………………	Work of outer volumetric forces (gravity force)
2nd term on the right	…………………	Thermodynamic reversible energy flux into the volume V and its change caused by pressure forces
3rd term on the right	…………………	Irreversible growth of energy due to dissipation caused by viscosity
4th term on the right	…………………	Vector of heat flux according to the Fourier law

The following equation is used for the calculations of species transport:

Species transport equation

In the model, time-averaged values of the local species mass fraction $\overline{Y}_{i'}$ are calculated. These values are described by a balance equation similar to the energy equation (see Equation 19). The energy equation includes both convective and diffuse components of the transport. It can be written in conservative form as

$$\frac{\partial}{\partial t}\left(\rho \cdot \overline{Y}_{i'}\right) + \frac{\partial}{\partial x_j}\cdot\left(\rho \cdot \overline{u}_j \cdot \overline{Y}_{i'}\right) = -\frac{\partial}{\partial x_i}J_{j,i'} + R_{i'} + S_{i'} \tag{20}$$

where $\overline{u}_j$ is the time-averaged j-coordinate of the flow field velocity [m/s], $R_{i'}$ is the production rate of species i' due to chemical reaction [kg/(m³.s)], and $S_{i'}$ is the growth production rate from distributed species [kg/(m³.s)]. The Equation (20) is valid for $N-1$ species, where N is the total number of components presented in the mathematical model [-]. Species distribution can be performed under various conditions, for which it can generally be divided into laminar and turbulent flow distribution. The value $J_{j,i'}$ represents the j-coordinate of i'-species diffuse flux [kg/(m³.s)]. To express the i'-species diffuse flux in the turbulent flow regime, the model employs

$$J_{i'} = -\left(\frac{\mu_t}{Sc_t}\right)\cdot\frac{\partial \overline{Y}_{i'}}{\partial x_j} \tag{21}$$

where μ_t is the turbulent dynamic viscosity [Pa.s], $\overline{Y}_{i'}$ is the time-averaged species i' mass fraction [-], and Sc_t is the Schmidt turbulent number [-] (set at the default value of 0.7) (see [1],[2]).

3.3. Example of numerical simulation – Gas pollutant motion in wind tunnel

ANSYS Fluent 13.0, one of the world's most sophisticated CFD codes, was chosen for the numerical simulation of the gas pollutant plume motion and dispersion. The gauging section of the low-speed wind tunnel with a small nozzle representing a chimney in a flat, simple terrain was the object of the numerical simulation. Gas pollutant enters the gauging section through the top of the nozzle (chimney) and is carried by flowing air (see Figure 3 to Figure 6).

Three-dimensional cubic geometry in five different model scales was designed for the purpose of this analysis (see Table 1).

The geometry grid at all modeled scales consisted of 569 490 three-dimensional cells. The problem was defined as steady (time-independent) with accuracy set at the value of 0.0001 (criterion of convergence).

RANS (Reynolds-averaged Navier-Stokes equations) approach was used for turbulent characteristics definition. RNG $k-\varepsilon$ model of turbulence was used for the air flow field basic calculation. The Boussinesq hypothesis of swirl turbulent viscosity was applied for the
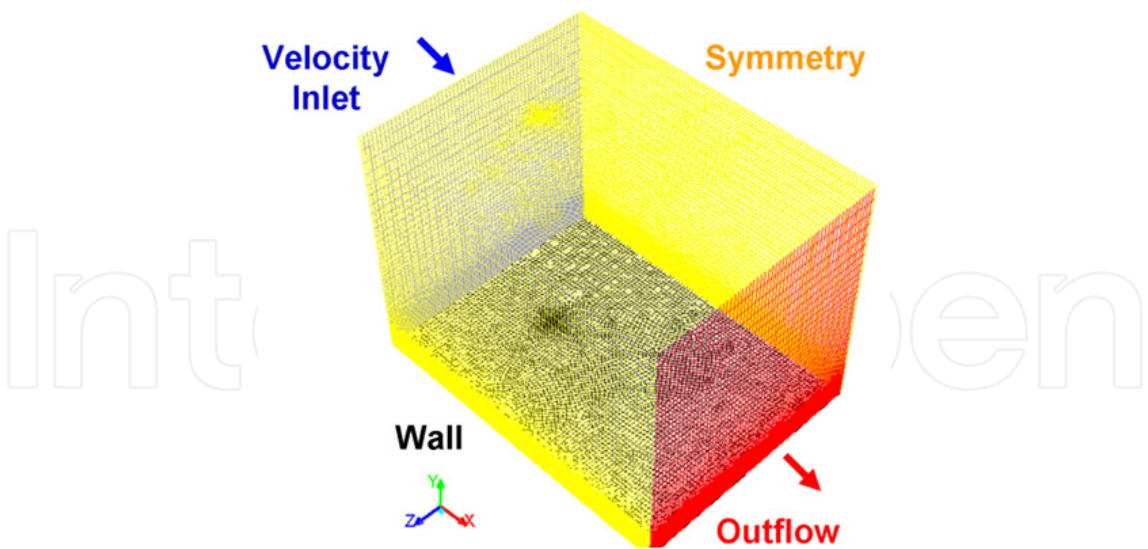
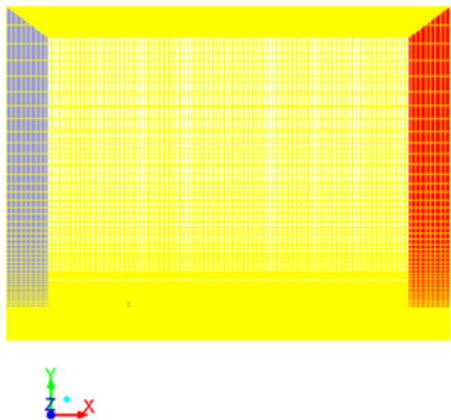**Figure 3.** Geometry and grid (isometric view)
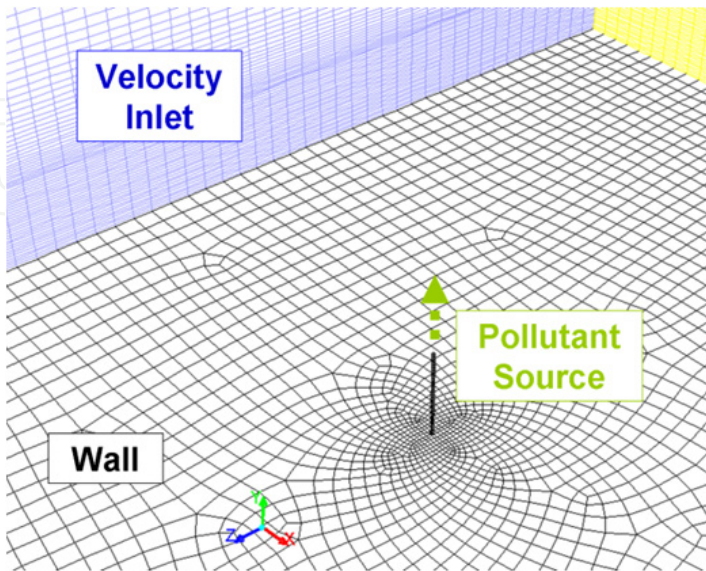

Figure 4. Geometry and grid (right side view)
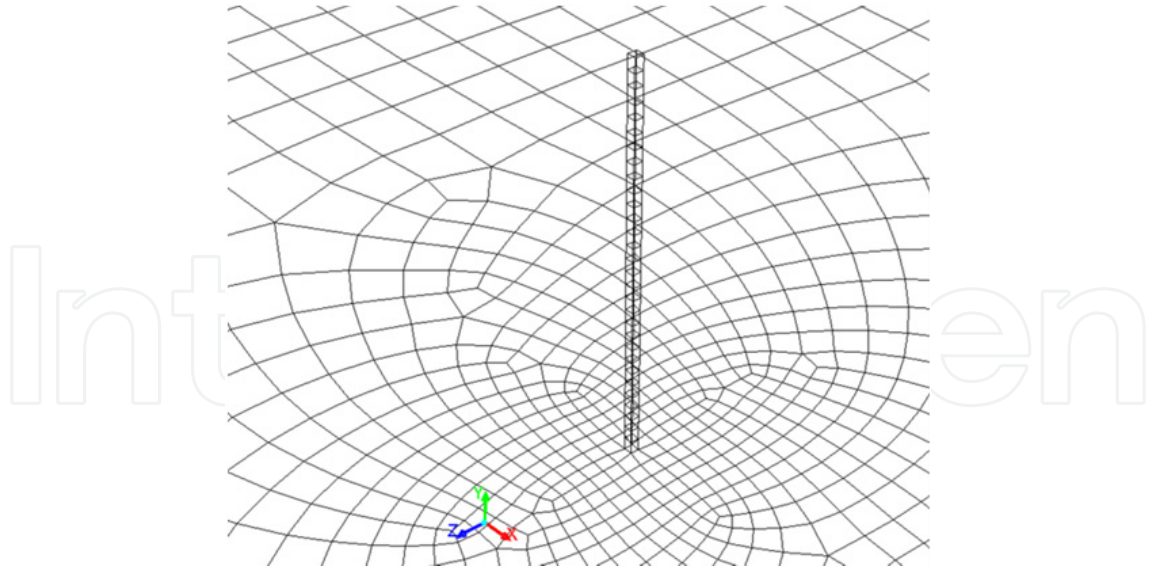

Figure 5. Pollutant source

Figure 6. Pollutant source (detail)

Model Scale [-]	Geometry Dimensions [m]	Nozzle (Chimney) Dimensions [m]	Nozzle (Chimney) Spout Surface [m]	Coordinates of the Nozzle (Chimney) [m]	Note
1:1	X = 2000 Y = 1500 Z = 1500	X = 3.5 Y = 200 Z = 3.5	X = 3.5 Z = 3.5	X = 500 Y = 0 Z = 750	Real Pattern
1:4.04	X = 495.04 Y = 371.28 Z = 371.28	X = 0.866 Y = 49.5 Z = 0.866	X = 0.866 Z = 0.866	X = 123.76 Y = 0 Z = 185.64	-
1:35.51	X = 56.32 Y = 42.24 Z = 42.24	X = 0.098 Y = 5.632 Z = 0.098	X = 0.098 Z = 0.098	X = 14.08 Y = 0 Z = 21.12	-
1:101.82	X = 19.64 Y = 14.73 Z = 14.73	X = 0.034 Y = 1.964 Z = 0.034	X = 0.034 Z = 0.034	X = 4.91 Y = 0 Z = 7.36	-
1:1000	X = 2.0 Y = 1.5 Z = 1.5	X = 0.0035 Y = 0.2 Z = 0.0035	X = 0.0035 Z = 0.0035	X = 0.5 Y = 0 Z = 0.75	Wind Tunnel

Table 1. Geometry dimensions and pollutant source coordinates by model scale

turbulent viscosity calculation (see [1],[2]). Species transport model was used for the species motion calculation. Both models worked simultaneously. No additional gas pollutant dispersion model was applied. The operating pressure was set at 101 325 [Pa], the operating temperature was 300 [K], and the gravity acceleration -9.81 [m/s²] in the geometry. Considering the pollutant source close surroundings, the ranges of the Reynolds number

Re were 250–1250 [-] (model scale 1:1000, referential air flow velocity 1–5 [m/s], and nozzle spout diameter 0.0035 [m]) and 250000–1250000 [-] (model scale 1:1, referential air flow velocity 1–5 [m/s], and chimney spout diameter 3.5 [m]).

Boundary conditions were set to *Velocity Inlet* at the inlet, *Outflow* at the outlet, *Wall* for the floor, *Symmetry* for the walls, *Wall* for pollutant walls, and *Velocity Inlet* for the nozzle (spout of the chimney).

Profiles of the flow field physical characteristics were determined at the inlet of the geometry (see Table 2) based on experimental data from a low-speed wind tunnel for a 1:1000-scale model (see [3],[4],[5],[11]). For other model scales, the profiles were modified to keep the trend of curves.

Title	*Equation*
Vertical profile of air flow velocity (X-direction)	$v_x = 0.2371 \cdot \ln\left(Y + 0.00327\right) + 1.3571$
Vertical profile of air turbulent intensity	$I = -0.0673 \cdot \ln\left(Y + 0.00327\right) + 0.1405$
Vertical profile of turbulent kinetic energy	$k = 1.5 \cdot \left(v_x \cdot I\right)^2$
Vertical profile of turbulent dissipation rate	$\varepsilon = \dfrac{1.225 \cdot 0.09 \cdot \left(k^3\right)}{1.4}$

Table 2. Air flow velocity profile and turbulent characteristics profiles in geometry

In Table 2 the parameter v_x represents the air flow velocity in the direction of X-axis [m/s], I is the intensity of turbulence [%], Y is the vertical coordinate of the geometry [m], k is the turbulent kinetic energy [m²/s²], and ε is the turbulent dissipation rate [m²/s³].

The pollutant source was designed as a nozzle (chimney) of a cuboid shape. Its dimensions and spout surfaces are shown in Table 1. For all model scales, the pollutant velocity $v_{polutant}$ was set at 0.5 [m/s], the intensity of turbulence in the pollutant source at 10 [%], the pollutant mass fraction in the pollutant source at 0.95 [-], and the air mass fraction in the pollutant source at 0.05 [-]. The hydraulic diameter of the pollutant source was set at 3.5 [m] for 1:1-scale model, 0.866 [m] for 1:4.04-scale model, 0.0986 [m] for 1:35.51-scale model, 0.344 [m] for 1:101.821-scale model, and 0.0035 [m] for 1:1000-scale model scale 1:1000.

Three different pollutants were chosen to be tested: helium, methanol and 1,2-dichlorethane. Helium ($\rho = 0.1625$ [kg/m³]) has a lower density than air, i.e., it is lighter than air ($\rho = 1.225$ [kg/m³]). Methanol ($\rho = 1.43$ [kg/m³]) has approximately the same density as air, i.e., it is approximately of the same weight as air. 1,2-dichlorethane ($\rho = 4.1855$ [kg/m³]) has a greater density than air, i.e., it is heavier than air. Plumes of pollutants lighter than air tend to climb, whereas those heavier than air tend to descend. However, this is not always the case. Pollutant plume vertical movements can be influenced by several other physical factors as demonstrated in the analysis (see Sections 2.4, 2.5 and 2.6).

3.4. Analysis of results by air flow velocity

The aim of this analysis is to compare gas pollutant plume shapes and motions for three different gas pollutants (helium, methanol and 1,2-dichlorethane) at different values of the air flow velocity v_{air}. The demonstration of the problem was performed with a 1:1-scale three-dimensional geometry representing the real pattern of a simple terrain with a chimney (see Table 1). The referential air flow velocities v_{air} at the level of the chimney spout (pollutant source) were 1 [m/s], 3 [m/s] and 5 [m/s].

The resulting values of the Froude number Fr for each pollutants and air flow velocities are shown in Table 3. Results were calculated using the ANSYS Fluent 13.0 software and were visualized as iso-surfaces of pollutant concentrations or as contours of pollutant concentration fields (see Figure 7 to Figure 12). The contours were plotted in two-dimensional planes of the geometry, sc., the central vertical longitudinal plane, the floor (ground) plane, and the outlet plane.

Pollutant	Chemical Symbol/Formula	Model Scale [-]	Air Flow Velocity [m/s]	Froude number [-]	Note
Helium (gas)	He	1 : 1	1	0.248	Fr < 1
		1 : 1	3	2.230	Fr > 1
		1 : 1	5	6.195	Fr > 1
Methanol (gas)	CH_3OH	1 : 1	1	0.028	Fr << 1
		1 : 1	3	0.253	Fr < 1
		1 : 1	5	0.704	Fr < 1
1,2-dichlorethane (gas)	CH_2ClCH_2Cl	1 : 1	1	0.010	Fr << 1
		1 : 1	3	0.088	Fr << 1
		1 : 1	5	0.246	Fr < 1

Table 3. Values of the Froude number for one model scale and three different air flow velocities

The following figures show that with increasing air flow velocity v_{air} the pollutant plume vertical movements are reduced. The pollutant plume inclines horizontally at the level of the chimney spout (pollutant source) showing no tendency to climb or descend. This is because the inertial force F_{I-air} increases as the air flow velocity v_{air} increases. Hence, the pollutant plume vertical movements are reduced or totally eliminated.

The air flow velocity also influences the size and shape of the pollutant plume. With increasing air flow velocity v_{air} the pollutant plume tends to be narrower and longer. However, a further increase in the air flow velocity makes the pollutant plume shorter because of greater rate of the pollutant dispersion. The plume range at certain concentration of the pollutant therefore decreases with increasing air flow velocity.
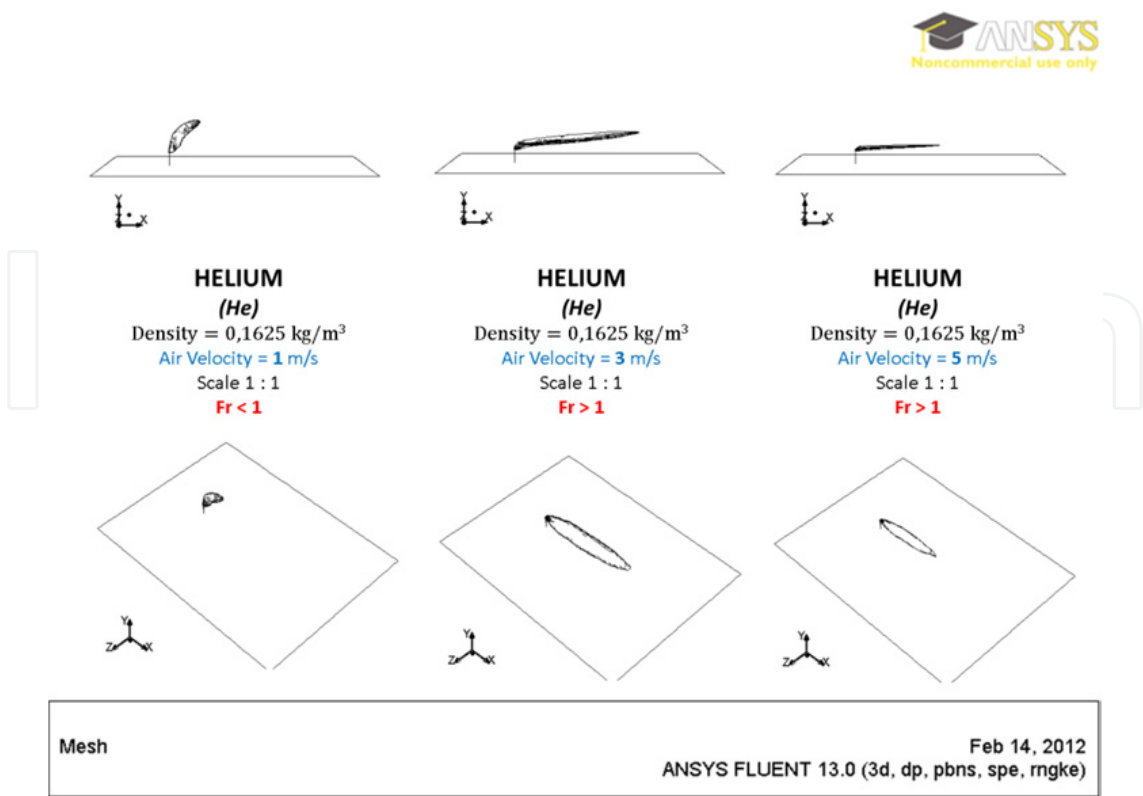
Figure 7. Gas pollutant plume motion analysis by air flow velocity (iso-surfaces of gaseous helium concentration with mass fraction of 0.0001 [-])
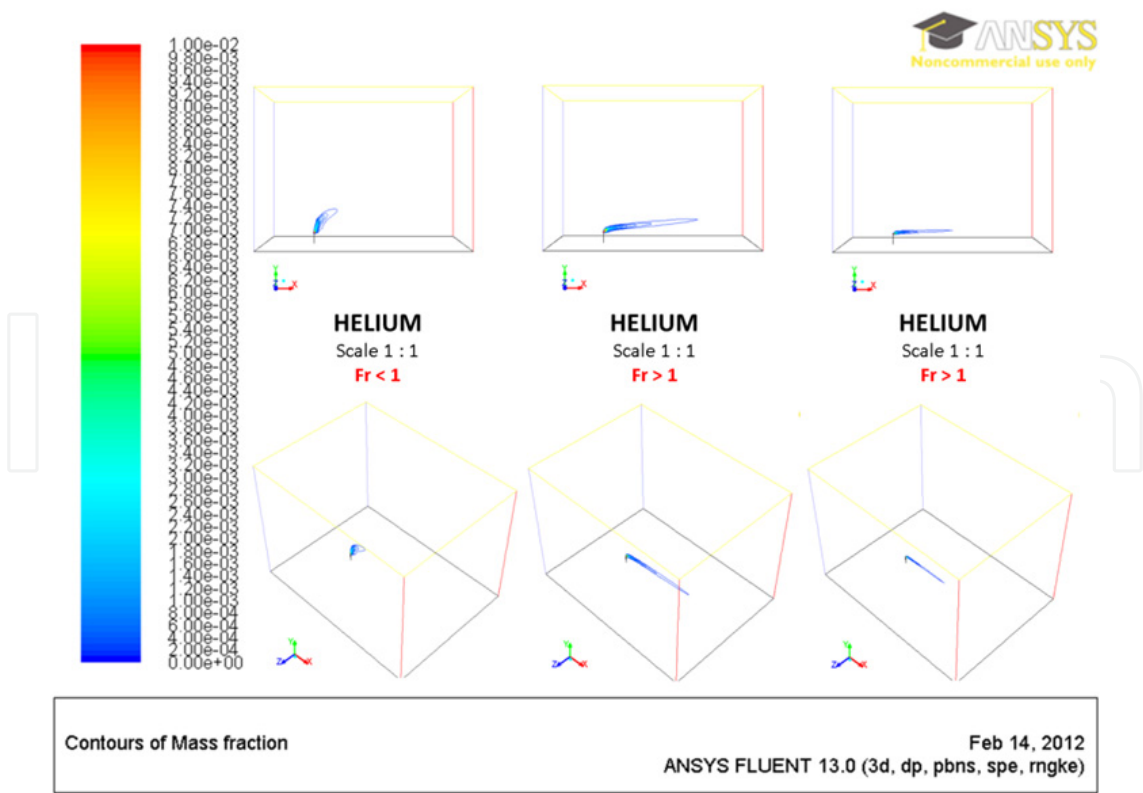

Figure 8. Gas pollutant plume motion analysis by air flow velocity (contours of gaseous helium concentration with mass fraction range of 0–0.01 [-])
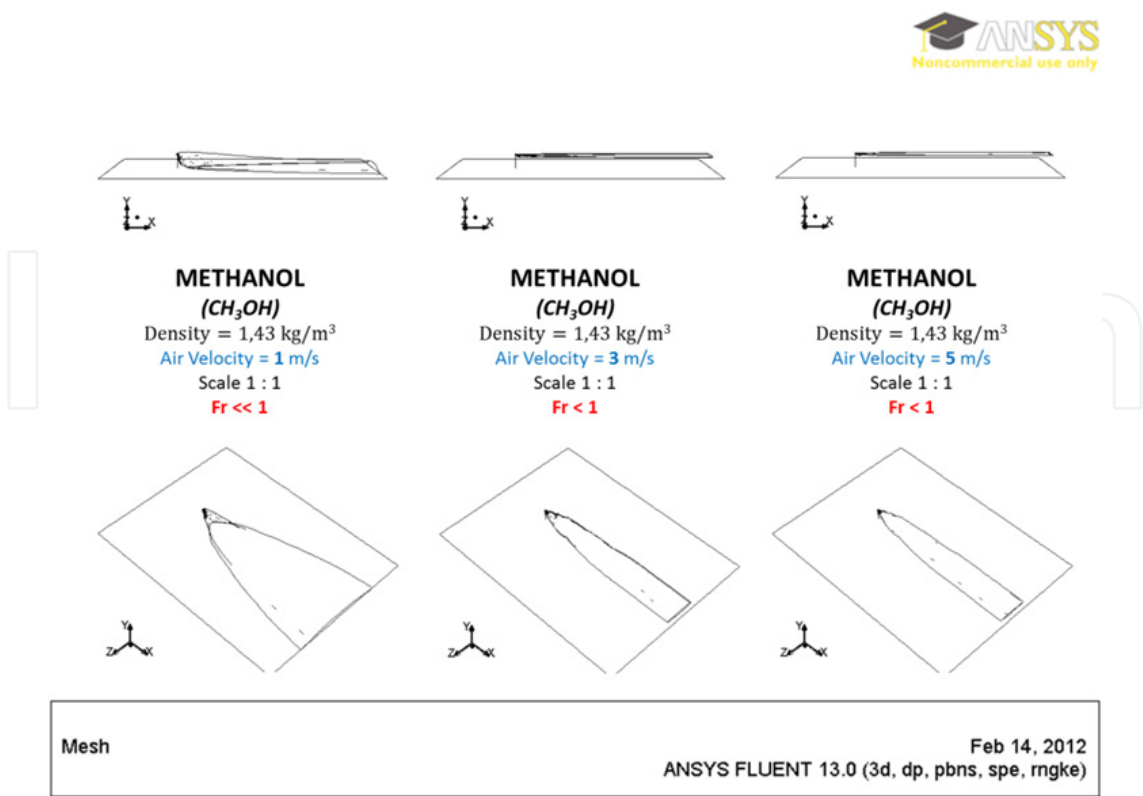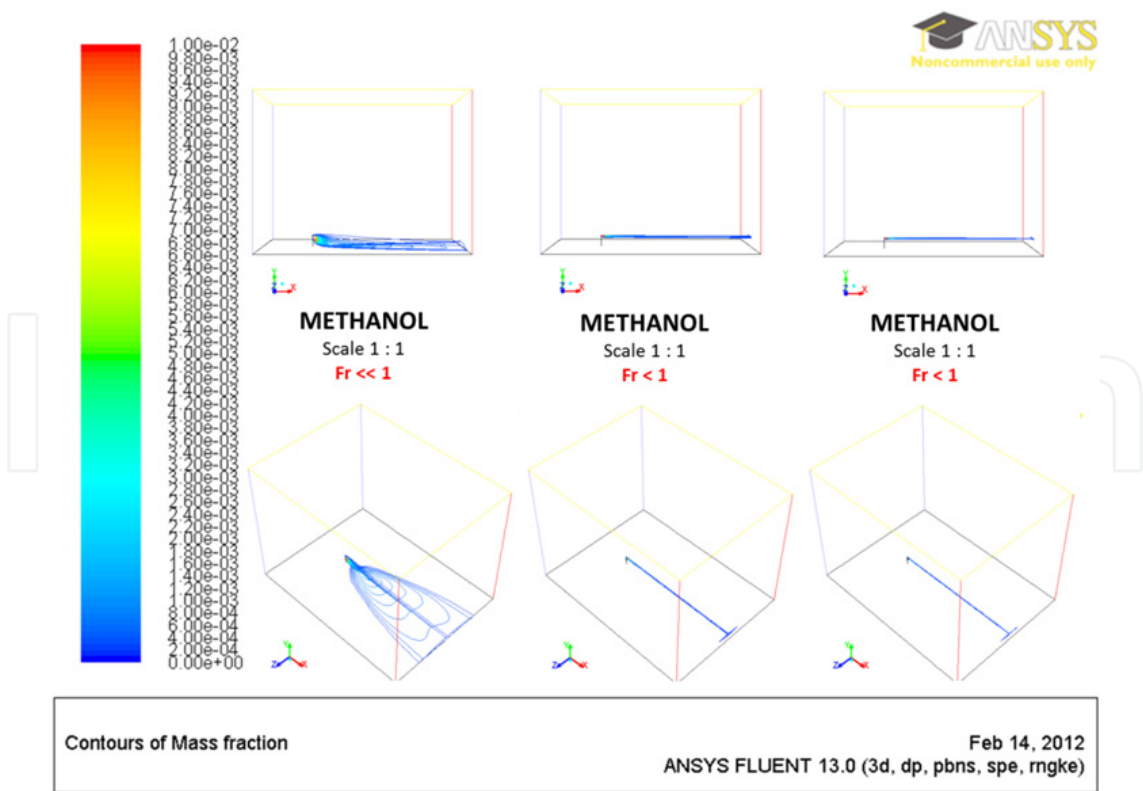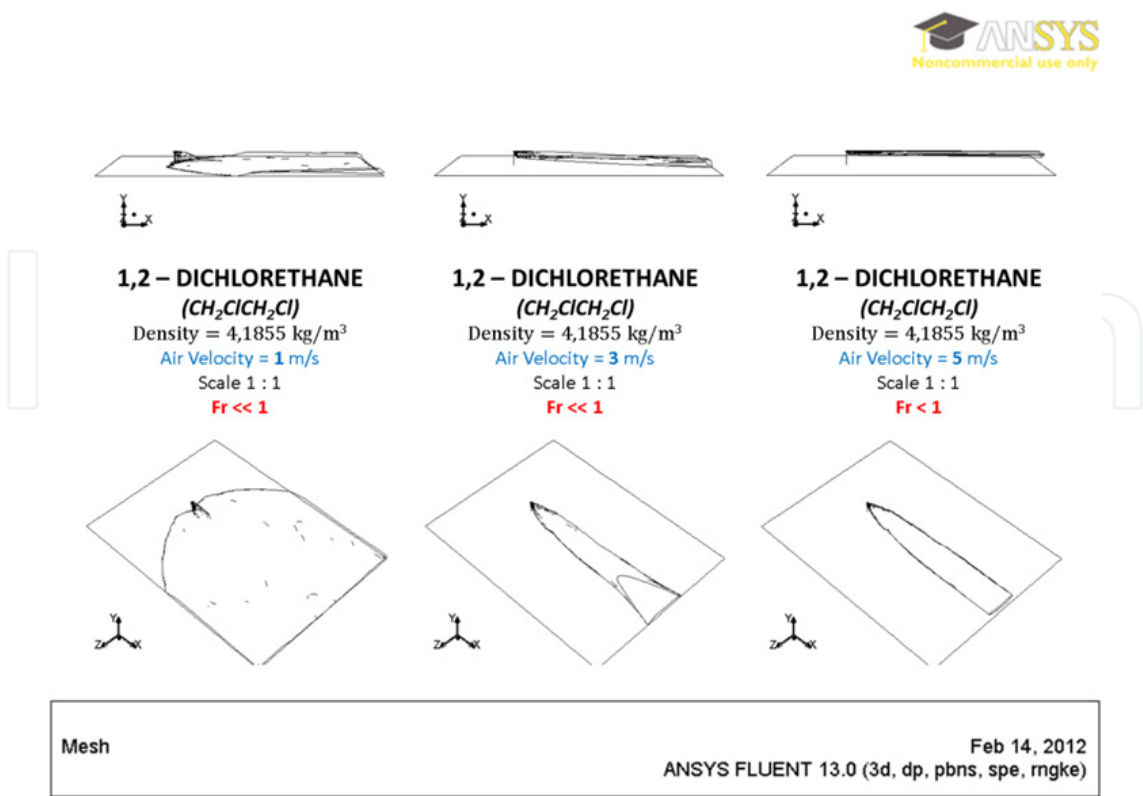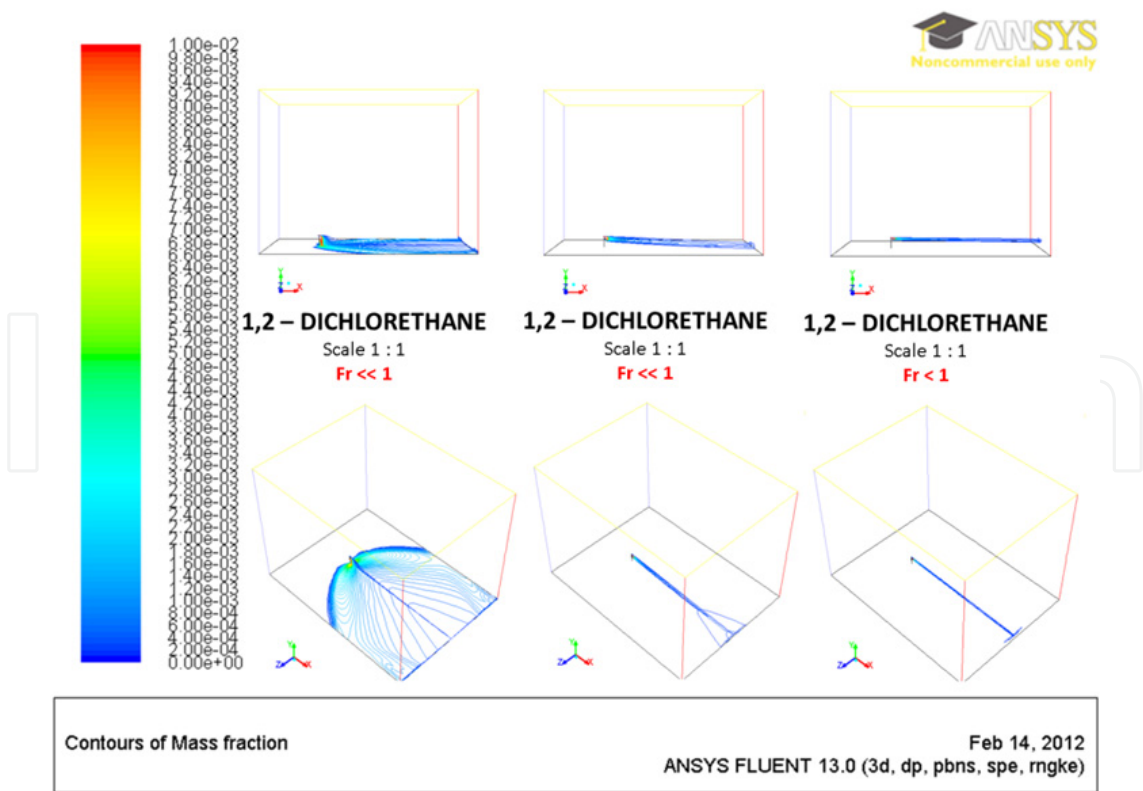
Figure 9. Gas pollutant plume motion analysis by air flow velocity (iso-surfaces of gaseous methanol concentration with mass fraction of 0.0001 [-])

Figure 10. Gas pollutant plume motion analysis by air flow velocity (contours of gaseous methanol concentration with mass fraction range of 0–0.01 [-])

Figure 11. Gas pollutant plume motion analysis by air flow velocity (iso-surfaces of gaseous 1,2-dichlorethane concentration with mass fraction of 0.0001 [-])

Figure 12. Gas pollutant plume motion analysis by air flow velocity (contours of gaseous 1,2-dichlorethane concentration with mass fraction range of 0–0.01 [-])

3.5. Analysis of results by pollutant density

The aim of this analysis is to compare gas pollutant plume shapes and motions for three different gas pollutants (helium, methanol and 1,2-dichlorethane) at different values of their density. Demonstration of the problem was performed with a 1:1-scale three-dimensional geometry representing the real pattern of a simple terrain with a chimney (see Table 1). The referential air flow velocity v_{air} at the level of the chimney spout (pollutant source) was 1 [m/s].

The resulting values of the Froude number Fr for each individual pollutant are shown in Table 4. Results were calculated using the ANSYS Fluent 13.0 software and were visualized as iso-surfaces of pollutant concentrations or as contours of pollutant concentration fields (see Figure 13 and Figure 14). The contours were plotted in two-dimensional planes of the geometry, sc., the central vertical longitudinal plane, the floor (ground) plane, and the outlet plane.

Pollutant	Chemical Symbol/Formula	Model Scale [-]	Air Flow Velocity [m/s]	Froude number [-]	Note
Helium (gas)	He	1 : 1	1	0.248	Fr < 1
Methanol (gas)	CH₃OH	1 : 1	1	0.028	Fr << 1
1,2-dichlorethane (gas)	CH₂ClCH₂Cl	1 : 1	1	0.010	Fr << 1

Table 4. Values of the Froude number for one model scale and one air flow velocity

The figures show that: If the pollutant density $\rho_{pollutant}$ is lower than the air density ρ_{air} the gas pollutant plume tends to climb (for helium see Figure 13 and Figure 14). If the pollutant density $\rho_{pollutant}$ is approximately the same as the air density ρ_{air} the gas pollutant plume neither climbs nor descends (for methanol see Figure 13 and Figure 14). If the pollutant density $\rho_{pollutant}$ is greater than the air density ρ_{air} the gas pollutant plume tends to descend (for 1,2-dichlorethane see Figure 13 and Figure 14). The range of vertical movements is determined by gravity force $F_{G-pollutant}$ that influences pollutant plume at given conditions. The greater the gravity force $F_{G-pollutant}$ is compared to the inertial force F_{I-air}, the more significant vertical movement of the plume is, i.e., light pollutant plume climbs and heavy pollutant plume descends.

The pollutant density $\rho_{pollutant}$ also influences the pollutant plume dispersion. The greater the pollutant density is, the longer the range of the plume is. At given air flow velocity v_{air}, the plume dispersion of pollutants with a low density is faster and easier than that of pollutants with a greater density.
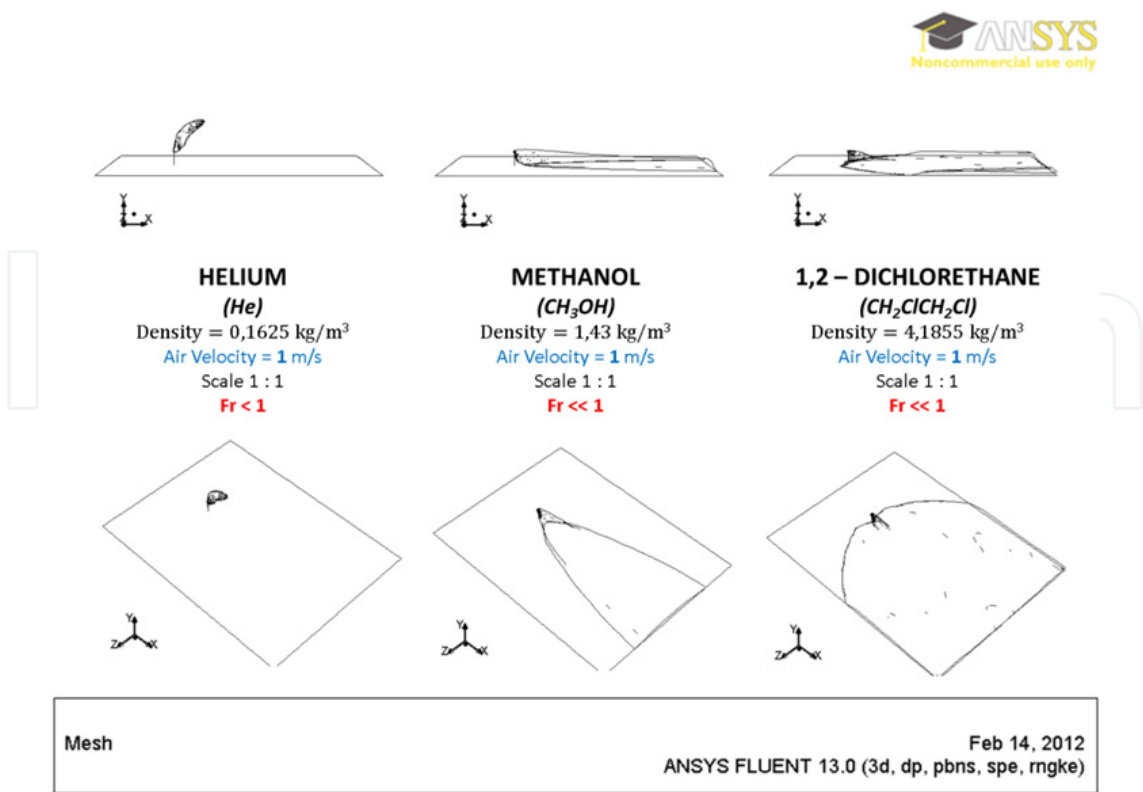
Figure 13. Gas pollutant plume motion analysis by pollutant density (iso-surfaces of gaseous helium, methanol, and 1,2-dichlorethane concentrations with mass fraction of 0.0001 [-]; 1:1-scale model)
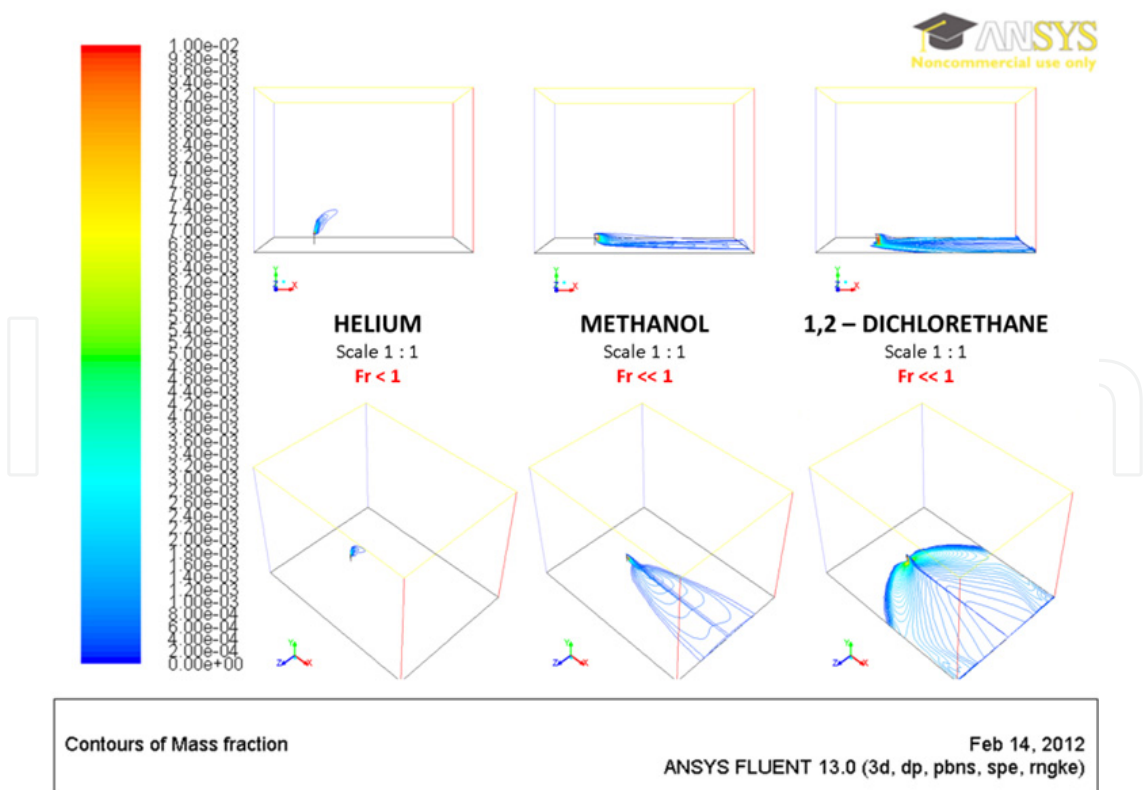

Figure 14. Gas pollutant plume motion analysis by pollutant density (contours of gaseous helium, methanol, and 1,2-dichlorethane concentrations with mass fraction range of 0–0.01 [-]; 1:1-scale model)

3.6. Analysis of results by model scale

The aim of this analysis is to compare gas pollutant plume shapes and motions for three different gas pollutants (helium, methanol, and 1,2-dichlorethane) at different model scales. The demonstration of the problem was performed with a three-dimensional geometry at three selected scales (see Table 1) for each of the three pollutants. The first 1:1-scale model represents the real pattern of a simple terrain with a chimney (pollutant source) where $Fr <$ 1, i.e., the gravity force $F_{G-pollutant}$ is greater than the inertial force F_{I-air}. The second model (scaled at 1:4.04, 1:35.51, and 101.82, respectively) represents the state when $Fr = 1$, i.e., the gravity force $F_{G-pollutant}$ equals the inertial force F_{I-air}. The third 1:1000-scale model represents the gauging section of a low-speed wind tunnel with a nozzle (pollutant source) on the floor where $Fr > 1$, i.e., the inertial force F_{I-air} is greater than the gravity force $F_{G-pollutant}$. The referential air flow velocity v_{air} at the level of the chimney spout (pollutant source) was 1 [m/s].

The resulting values of the Froude number Fr for each pollutant and model scale are shown in Table 5. Results were calculated using the ANSYS Fluent 13.0 software and were visualized as iso-surfaces of pollutant concentration or as contours of pollutant concentration fields (see Figure 15 to Figure 20). Contours were plotted in two-dimensional planes of the geometry, sc. the central vertical longitudinal plane, the floor (ground) plane, and the outlet plane.

Pollutant	Chemical Symbol/Formula	Model Scale [-]	Air Flow Velocity [m/s]	Froude number [-]	Note
Helium (gas)	He	1 : 1	1	0.248	Fr < 1
		1 : 4.04	1	1	Fr = 1
		1 : 1000	1	247.806	Fr >> 1
Methanol (gas)	CH₃OH	1 : 1	1	0.028	Fr << 1
		1 : 35.51	1	1	Fr = 1
		1 : 1000	1	28.160	Fr >> 1
1,2-dichlorethane (gas)	CH₂ClCH₂Cl	1 : 1	1	0.010	Fr << 1
		1 : 101.82	1	1	Fr = 1
		1 : 1000	1	9.822	Fr > 1

Table 5. Values of the Froude number for different model scales and one air flow velocity

The figures (see Figure 15 to Figure 20) show that: If the model scale changes and all other characteristics remain unchanged, the inertial and gravity forces and their ratio change too. Therefore, the size, shape and inclination of the pollutant plume change.

According to Equation (11) in Section 1.5, the inertial force is proportional to the square of the model scale. According to Equation (12) in Section 1.5, the gravity force is proportional to the third power of the model scale. Therefore, the change in the gravity force due to the change of the model scale is considerably greater than the change in the inertial force. The lower the model scale is, the greater the dominance of inertial forces is compared to gravity forces), and vice versa.

Also, the greater the pollutant density, the lower the model scale is if $Fr = 1$, i.e., the inertial and gravity forces are equal.
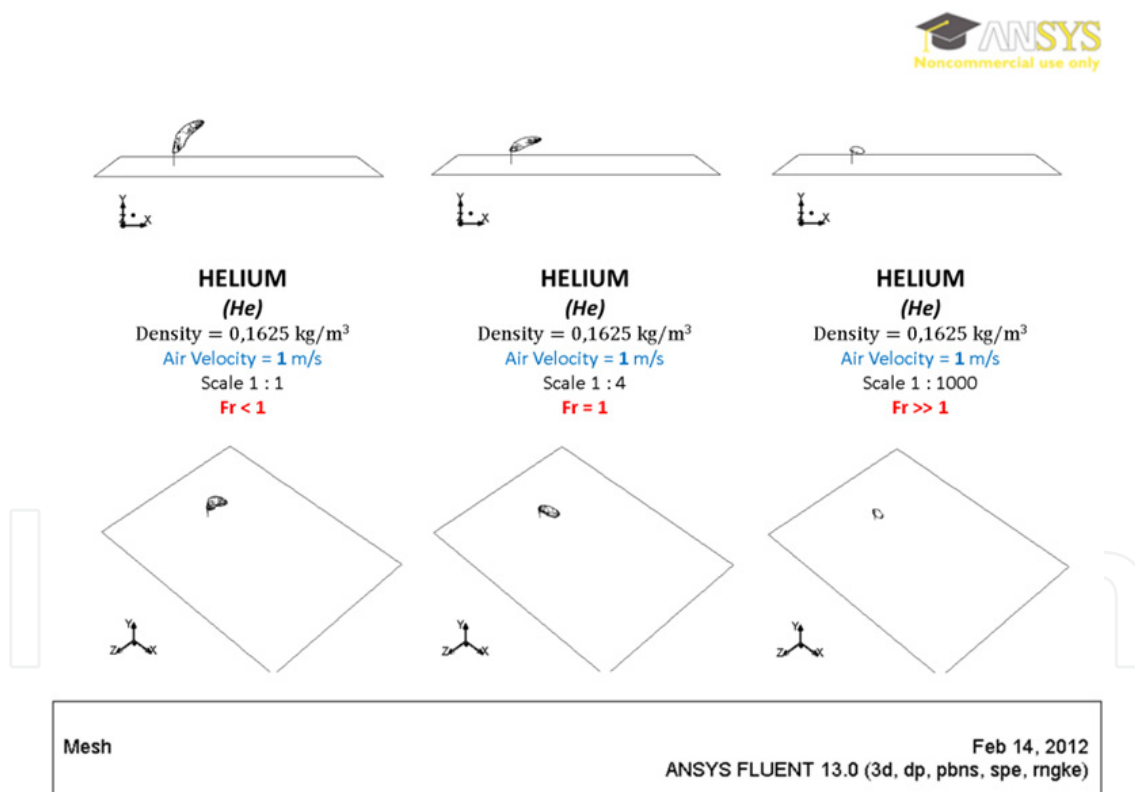

Figure 15. Gas pollutant plume motion analysis by model scale (iso-surfaces of gaseous helium concentration with mass fraction of 0.0001 [-] for three different model scales)
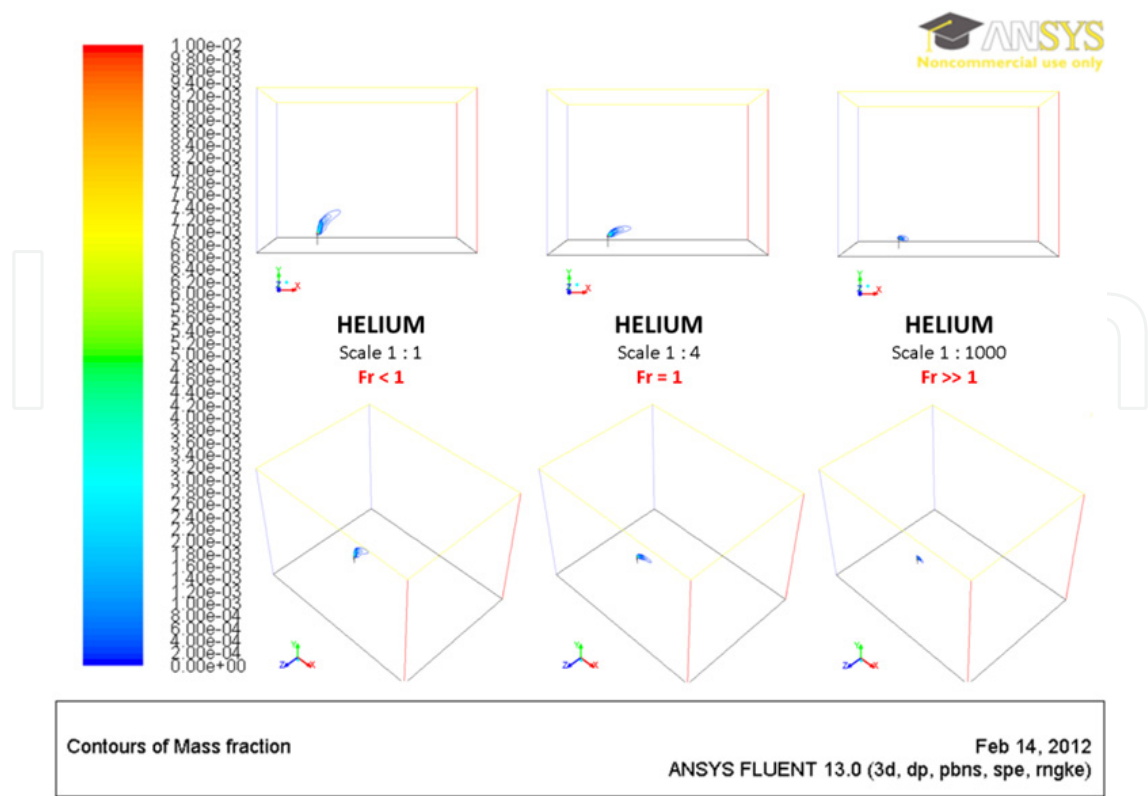
Figure 16. Gas pollutant plume motion analysis by model scale (contours of gaseous helium concentration with mass fraction range of 0–0.01 [-] for three different model scales)
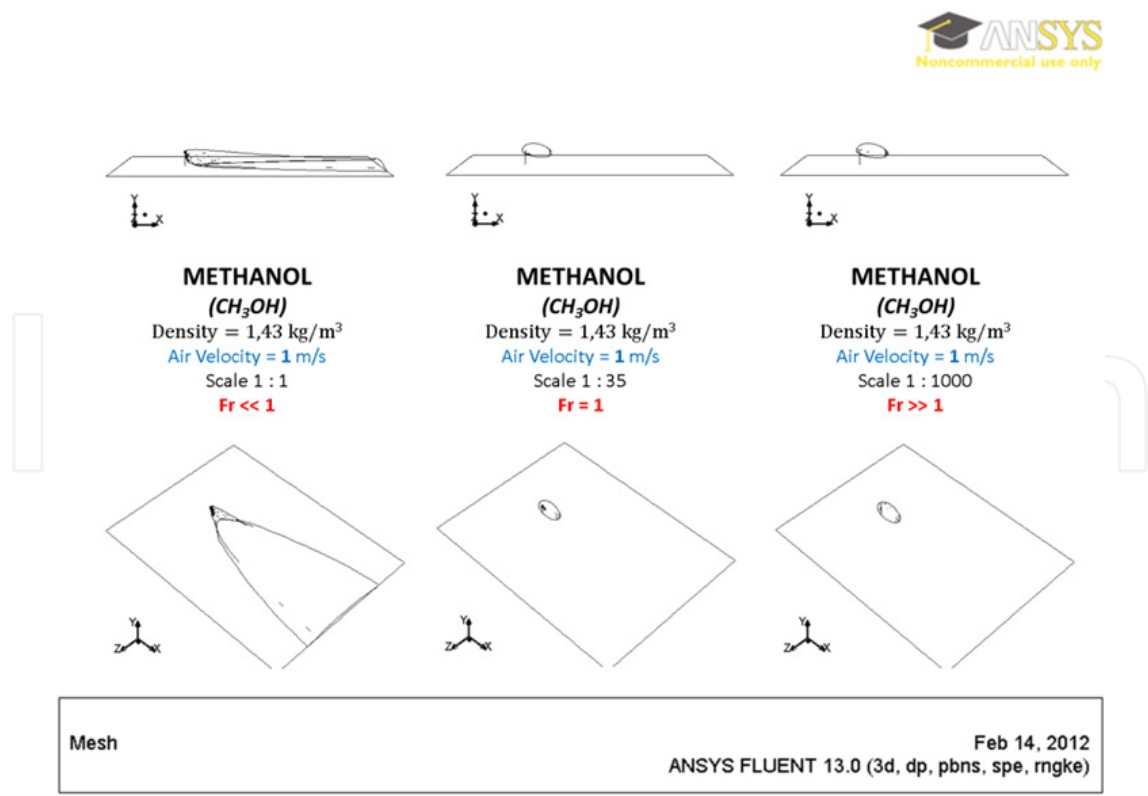

Figure 17. Gas pollutant plume motion analysis by model scale (iso-surfaces of gaseous methanol concentration with mass fraction of 0.0001 [-] for three different model scales)
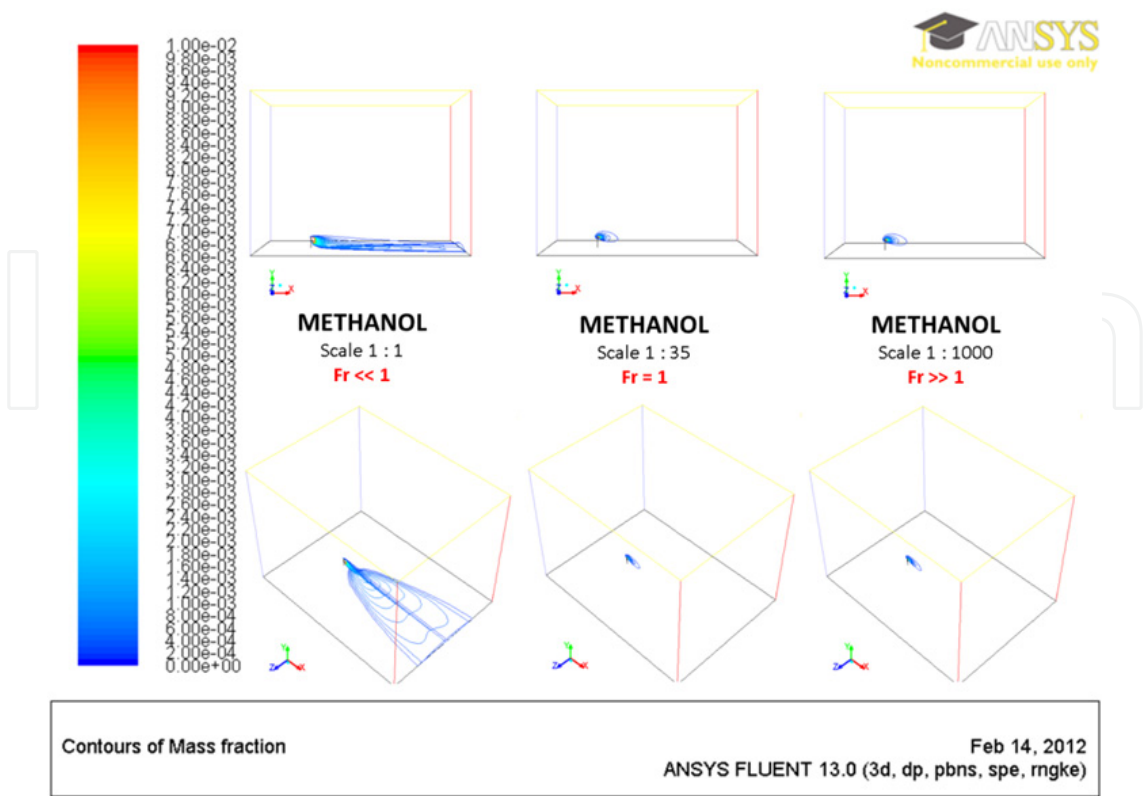
Figure 18. Gas pollutant plume motion analysis by model scale (contours of gaseous methanol concentration with mass fraction range of 0–0.01 [-] for three different model scales)
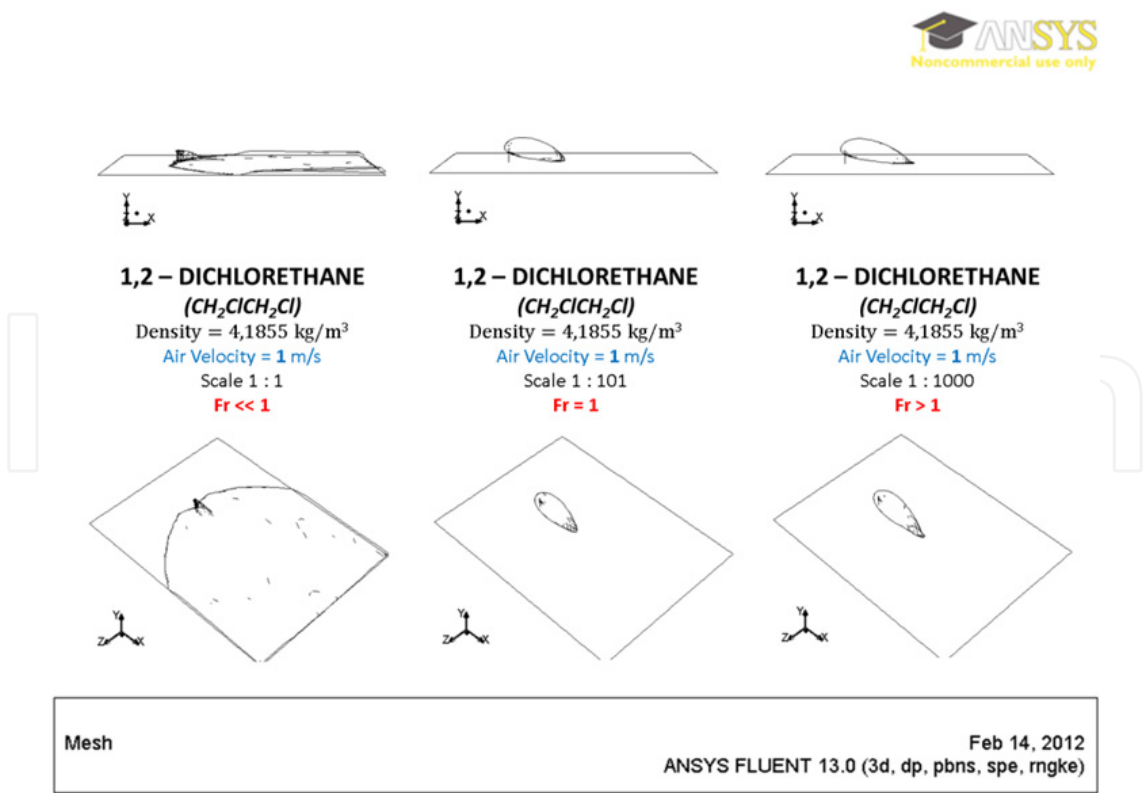

Figure 19. Gas pollutant plume motion analysis by model scale (iso-surfaces of gaseous 1,2-dichlorethane concentration with mass fraction of 0.0001 [-] for three different model scales)
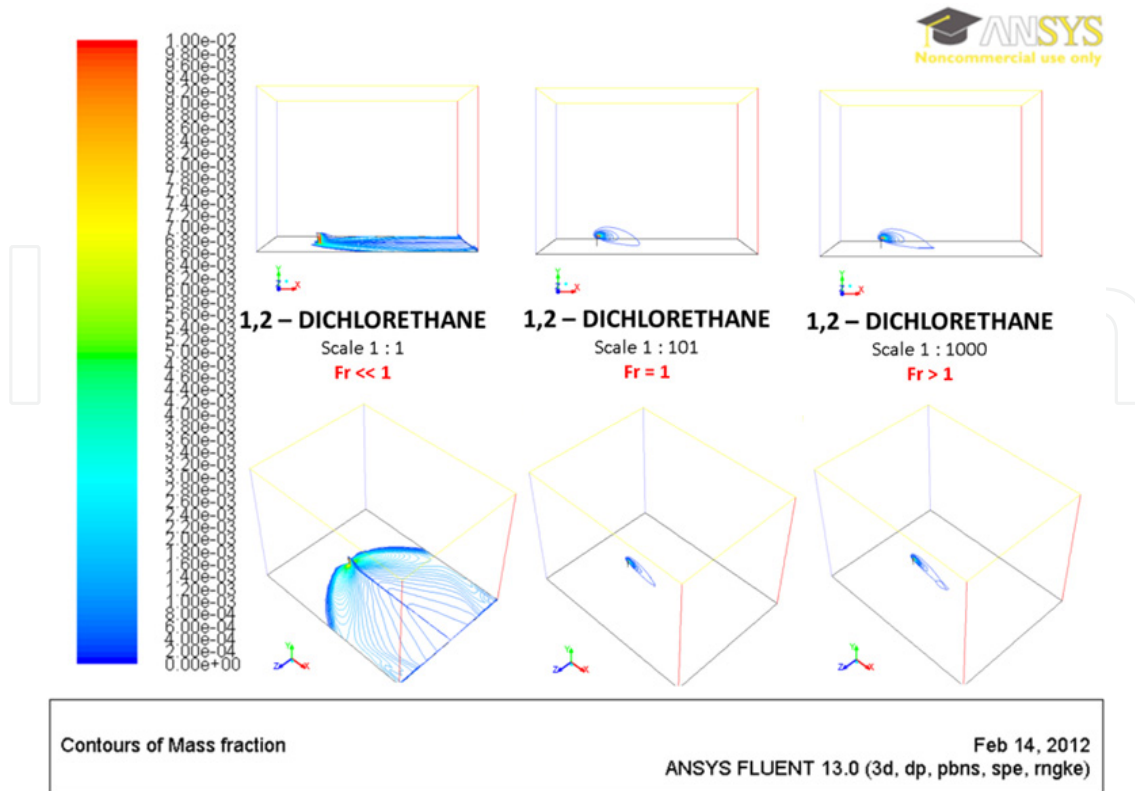
Figure 20. Gas pollutant plume motion analysis by model scale (contours of gaseous 1,2-dichlorethane concentration with mass fraction range 0–0.01 [-] for three different model scales)

4. Conclusion

The aim of the analyses was to lay down principles for physical and mathematical modeling of gas pollutant plume motion and dispersion in real atmospheric conditions. The influences of the air flow velocity, pollutant's density, and model scale on pollutant plume size, shape, and inclination were investigated.

The Froude number was chosen as a criterion of physical similarity for the pollutant plume behavior in the atmosphere. Basic mathematical rules and principles (see Chapter 1) were formulated upon study of available fluid mechanics literature (see [7],[8],[9],[10],[11]). All mathematical and physical assumptions were next verified by numerical simulation using the ANSYS Fluent 13.0 software. Air flow field was modeled using the RNG $k - \varepsilon$ model of turbulence, the gas pollutant motion was modeled using the Species Transport Model, both in the same three-dimensional geometry consisting of 569 490 grid cells. Turbulent characteristics were defined using RANS approach. No additional dispersion model was applied (see Chapter 2).

Object of modeling was gauging section of the low speed wind tunnel (for model scale of 1:1000) or big real terrain (for model scale of 1:1) with a pollutant source in form of nozzle (or chimney, respectively) situated on the section floor (ground). The gauging section with the nozzle represented a chimney in a simple, flat terrain. The chimney was considered to be a pollutant source for three different gas pollutants (helium, methanol, and 1,2-

dichlorethane). The numerical simulation was performed for five model scales, three gas pollutants with different densities, and three different air flow velocities. The simulations were steady (time-independent) with the accuracy of 0.0001 (criterion of convergence). Final results were visualized as iso-surfaces of pollutant concentrations and contours of pollutant concentration fields with the concentration limit value of 0,001. The contours were plotted in two-dimensional planes of the geometry, sc. the central vertical longitudinal plane, the floor (ground) plane and the outlet plane. The numerical model had been verified by an experiment performed in a low-speed wind tunnel (see [3],[4],[5]).

The following principles based on the results of the Froude number analysis of pollutant plume motion and dispersion in real atmosphere can be defined:

1. The greater the air flow velocity is, the greater the inertial forces are. These forces influence pollutant plume and reduce its vertical motions (inclination). With increasing air flow velocity the pollutant plume inclines horizontally at the level of the chimney spout (pollutant source), but with further increase in the air flow velocity it becomes narrower and shorter (see Section 2.4).

2. The greater the difference between pollutant density and air density is, the more significant the tendency towards vertical movements (climbing or descending) of the plume is. The plume of pollutant with lower density than air tends to climb, whereas the plume of pollutant with greater density than air tends to descend. The density of the pollutant also influences the pollutant plume dispersion. The greater the pollutant density is, the longer the range of the plume is. At given air flow velocity v_{air}, the plume dispersion of pollutants with a low density is faster and easier than that of pollutants with a greater density (see Section 2.5).

3. If the model scale changes and all other characteristics remain unchanged, the inertial and gravity forces and their ratio change too. Therefore, the size, shape and inclination of the pollutant plume change. The inertial force is proportional to the square of the model scale, whereas the gravity force is proportional to the third power of the model scale (see Section 1.5). The change in the gravity force due to the change of model scale is considerably greater than the change in the inertial force. The lower the model scale is, the greater the dominance of inertial forces is compared to gravity forces. Also, the greater the pollutant density is, the lower the model scale is if $Fr = 1$, i.e., the inertial and gravity forces are equal (see Section 2.6).

From the above it follows that if investigators want to respect and follow the basics of physical phenomena, they must consider criteria of physical similarity very carefully, in particular criteria of dynamic similarity (see Section 1.1). Some physical phenomena, however, cannot be modeled in any model scale but the original one without changing the basis of the phenomena (see Sections 1.5 and 2.6).

This analysis is intended for those who are interested in gas pollutant plume motion in the atmosphere and in theory of physical similarity. The conclusions of the analysis can be used for further experiment design works or for checking results of mathematical modeling.

Author details

Ondrej Zavila

Vysoka Skola Banska, Technical University of Ostrava, Faculty of Safety Engineering, Ostrava, Vyskovice, Czech Republic

Acknowledgement

5. References

[1] Kozubkova M (2008) Modeling of Fluid Flow (in Czech), FLUENT, CFX. Ostrava: VSB - Technical University of Ostrava. 153 p.

[2] Bojko M (2008) Guide for Training of Flow Modeling – FLUENT (in Czech). Ostrava: VSB - Technical University of Ostrava. 141 p.

[3] Civis S, Zelinger Z, Strizik M, Janour Z (2001) Simulation of Air Pollution in a Wind Tunnel. Spectroscopy from Space. Dordrecht: Kluwer Academic. pp. 275-299

[4] Zelinger Z, Strizik M, Kubat P, Janour Z, Berger P, Cerny A, Engst P (2004) Laser Remote Sensing and Photoacoustic Spectrometry Applied in Air Pollution Investigation. Opt. Lasers Eng. 42. pp. 403-412

[5] Zelinger Z, Strizik M, Kubat P, Civis S, Grigorova E, Janeckova R, Zavila O, Nevrly V, Herecova L, Bailleux S, Horka V, Ferus M, Skrinsky J, Kozubkova M, Drabkova S, Janour Z (2009) Dispersion of Light and Heavy Pollutants in Urban Scale Models: CO_2 Laser Photoacoustic Studies. Applied spectroscopy. Society for Applied Spectroscopy. pp. 430-436.

[6] Benson, Tom (2010) Wind Tunnel Index. Available: http://www.grc.nasa.gov/WWW/k-12/airplane/shortt.html. Accessed 2012 March 4.

[7] Carnogurska M, Prihoda M (2011) Application of Three-dimensional Analysis for Modelling Phenomena in the field of Power Engineering (in Slovak). Kosice: Technical University of Kosice. 214 p.

[8] Incropera F.P, Dewitt D.P, Bergman T.L, Lavine A.S (2007) Fundamentals of Heat and Mass Transfer. New York: John Wiley & Sons. 997 p.

[9] Shaughnessy E.J, Katz M.I, Schaffer J.P (2005) Introduction to Fluid Mechanics. New York: Oxford University Press. 1118 p.

[10] Drabkova S, Platos P (2003) Numerical Simulation as a Tool for the Solution and Understanding of Practical Air Pollution Problems. Proc. of the Conference on Modelling Fluid Flow (CMFF'03). Budapest: Budapest University of Technology and Economics. pp. 501-506.

[11] Stull B.R (1994) An Introduction to Boundary Layer Meteorology. Dordrecht: Kluwer Academic Publisher. 666 p.